



# Structural differences between chitin polymorphs and their precipitates from solutions — evidence from CP-MAS $^{13}\text{C}$ -NMR, FT-IR and FT-Raman spectroscopy

B. Focher

Stazione Sperimentale Cellulosa, Piazza Leonardo da Vinci 26, 20133 Milano, Italy

A. Naggi, G. Torri

Istituto Scientifico di Chimica e Biochimica 'G. Ronzoni', Via G. Colombo, 81, 20133 Milano, Italy

A. Cosani & M. Terbojevich

Centro Biopolimeri, CNR, Dipartimento di Chimica Organica, Università di Padova, Via Marzolo 1, 35131 Padova, Italy

(Received 13 September 1990; revised version received 3 December 1990; accepted 10 January 1991)

Structural differences between  $\alpha$ -chitin from shrimp (*Crangon crangon*) and  $\beta$ -chitin from squid (*Loligo*), as well as between their precipitated products from N,N-dimethylacetamide-LiCl solutions, are indicated by the CP-MAS  $^{13}\text{C}$ -NMR, FT-IR, FT-Raman spectra and the X-ray diffractograms.

The  $^{13}\text{C}$ -NMR spectra in the solid state of  $\alpha$ -chitin consisting of eight major resonances suggest a high degree of structural homogeneity. In the spectrum of  $\beta$ -chitin, the C-3 and C-5 signals merged in a single resonance.

The bands contour of deconvoluted and curve-fit FT-IR and FT-Raman spectra shows a more detailed structure of  $\alpha$ -chitin in the region of O—H, N—H and C=O stretching regions; in particular the Amide I band is split, whereas a single broad band dominates in the corresponding  $\beta$ -form.

Precipitation treatments induce a general disorder in  $\alpha$ -chitin, while the metastable structure of  $\beta$ -chitin tends toward a more ordered architecture.

All the present spectroscopic data of chitin samples are consistent with the corresponding X-ray diffraction patterns.

## INTRODUCTION

Chitin, a linear polysaccharide composed of  $\beta$ -(1-4) linked 2-deoxy-2-acetamido-D-glucose units, forms the exoskeleton of invertebrates and one of the components of the cell wall of fungi (Muzzarelli, 1977; Muzzarelli *et al.*, 1986). It occurs naturally in three polymorphic forms known as  $\alpha$ -,  $\beta$ - and  $\gamma$ -chitin (Rudall, 1963).

The crystal structure of chitin has been studied mainly by use of X-ray diffraction and infrared spectroscopy. X-ray studies (Calstrom, 1957; Dwelz, 1960; Blackwell, 1969; Ramakrishnam & Prasad, 1972; Gardner & Blackwell, 1975; Abdul-Haleem & Parker, 1976; Minke & Blackwell, 1978) showed that the three forms of chitin differ in the packing and polarities of

adjacent chains in successive sheets; in the  $\beta$ -form all chains are aligned in parallel manner, whereas in  $\alpha$ -chitin they are antiparallel. IR studies established differences both in the hydrogen bonding network and in the Amide I vibration mode (Darmon & Rudall, 1950; Pearson *et al.*, 1960; Gow *et al.*, 1987).

In the present work,  $\alpha$ - and  $\beta$ -chitins and the products obtained by precipitation from N,N-dimethylacetamide-LiCl solutions have been characterized by CP-MAS  $^{13}\text{C}$ -NMR, FT-IR and FT-Raman spectroscopy. The precipitated forms have been included in this study owing to the ability of chitin to form mesophases in suitable solvent systems (Terbojevich *et al.*, 1988), hence to give high modulus fibers and films after precipitation.

## EXPERIMENTAL

### Materials and methods

A commercial sample of  $\alpha$ -chitin ( $\eta$  55 dl/g, mol. wt  $2.0 \times 10^6$ , Ac 100%) from shrimp (*Crangon crangon*) was supplied by Chito-Bios srl (Italy).  $\beta$ -Chitin ( $\eta$  50 dl/g, mol. wt  $1.8 \times 10^6$ , Ac 95%) was extracted in the authors' laboratory from the pens of Loligo squid. To obtain a protein-free product,  $\beta$ -chitin was purified with 1.0 NaOH solution for 24 h at room temperature and then with 0.15 mg/ml pepsin (EC 3.4.23) in  $10^{-3}$  M acetic acid solution at 37°C for 16 h. Both chitin polymorphs were dissolved in N,N-dimethylacetamide (DMAc) containing 5% LiCl and precipitated with water. Then, the precipitates ( $\alpha_p$  and  $\beta_p$ ) were washed with water and the complete elimination of LiCl was verified by atomic absorption spectroscopy. The samples ( $\alpha_p$ : Ac = 100%;  $\beta_p$ : Ac = 98%) were recovered by lyophilizing the slurry.

The degree of acetylation (Ac%) was determined by elemental analysis on the dried samples (105°C, 24 h). The intrinsic viscosity ( $\eta$ ) measurements were made in DMAc-LiCl (5%) at  $25.0 \pm 0.1$ °C, using a suspended level Ubbelohde viscometer. Molecular weights were evaluated from relationship ( $\eta$ )/mol. wt in DMAc-LiCl (Terbojevich *et al.*, 1988).

### X-Ray diffractometry

The X-ray powder patterns were recorded using Ni-filtered CuK $\alpha$ -radiation from a Siemens (Munich) 500 D diffractometer equipped with a scintillator counter and a linear amplifier.

### CP-MAS $^{13}\text{C}$ -NMR spectroscopy

The CP-MAS  $^{13}\text{C}$ -NMR spectra were obtained with a Bruker (Karlsruhe) CXP-300 (75 MHz) spectrometer. The cross polarization time was 1 ms, while the repetition time and the  $^1\text{H}$  90° pulse were 10 s and 3.5°  $\mu\text{s}$ , respectively. The full width at half-height of the reference glycine was 27 MHz. The chemical shifts were measured with respect to trimethylpropionic acid sodium salt (TSP). Scans (500–3000) were taken; the rotational speed was about 3.4 kHz.

### FT-IR spectroscopy

The infrared spectra were obtained with a Bruker (Karlsruhe) IFS 66 FT-IR spectrometer, using KBr pellets prepared according to Abbot *et al.* (1988). The reproducibility of the spectra was verified on two preparations of ground samples. Deuteration treatments were carried out by dispersing the mixture of the sample and KBr powder in D $_2$ O for 24 h. Between 16 and 100 scans were taken with a resolution of 4 cm $^{-1}$ .

In order to visualize some details in band shape and in the unresolved band components, Fourier self-deconvolution (FDS) and Fourier derivation (FD) procedures were applied, using a Bruker software making use of methods of Kauppinen (1981) and Susi and Byler (1983), respectively. Unresolved bands became apparent provided that their separation was greater than the instrumental resolution. Values of 13–15 cm $^{-1}$  for the half-width Lorentzian line and 1.3 for the resolution enhancement factor (Kauppinen *et al.*, 1981) avoided side lobes and preserved the constancy of band areas of samples. Smoothing of the second derivative spectra was accomplished prior to plotting with a nine-point Savitsky and Golay (1964) function. The signal-to-noise ratio was better than 500. The best quantitative information was obtained from the fitting of deconvoluted spectra (Griffiths, 1983; Thomas & Agard, 1984) using 'Fit', a Fortran program in the Bruker software, which makes use of an iterative procedure.

### FT-Raman spectroscopy

The Raman spectra were obtained with a Bruker FRA 106 Raman accessory for IFS 66 FTIR spectrometer using a laser excitation at 1064 nm (Nd : YAG laser, power 0.2 W). The 180° scattering arrangement was used and no correction for the spectral response of the instrument was applied. One hundred scans were taken with a resolution of 4 cm $^{-1}$ .

## RESULTS AND DISCUSSION

### $\alpha$ - and $\beta$ -chitins

The CP-MAS  $^{13}\text{C}$ -NMR spectrum of  $\alpha$ -chitin (Fig. 1) is similar to the spectra of shrimp (Gagnaire *et al.*, 1978) and crab shell (Saito *et al.*, 1987) and consists of eight well-defined resonances indicating a high structural homogeneity which parallels the high order degree suggested by the line width of signals. In the corresponding spectrum of  $\beta$ -chitin (Fig. 1), the signals of C-3 and C-5 carbons merge into a single resonance centered at 77 ppm, which causes a chemical shift variation of C-3 suggesting involvement of this carbon in a new structural feature.

Similarly, the X-ray powder diffractograms (not shown) reveal for  $\alpha$ -chitin a detailed structure with the presence of various equatorial reflections, as well as of highly perfect crystals, likely associated with a regular chain packing.

The disappearance in the diffractogram of  $\beta$ -chitin of the (020) reflection, associated with the most ordered regions involving the acetamido groups (Focher *et al.*, 1992), suggests different packing of chains and/or a

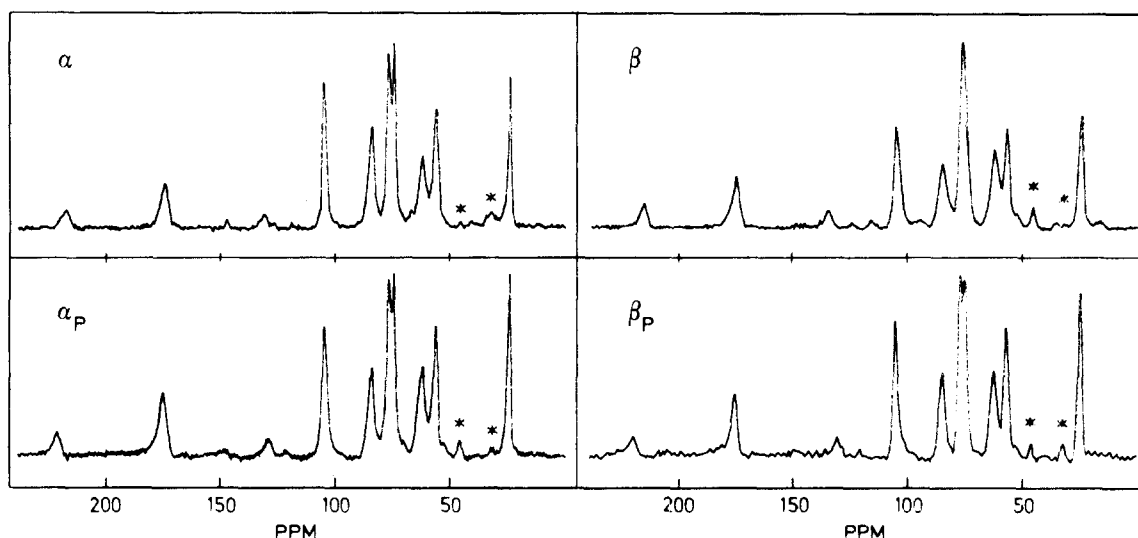


Fig. 1. CP-MAS  $^{13}\text{C}$ -NMR spectra of  $\alpha$ -,  $\beta$ -,  $\alpha_p$ - and  $\beta_p$ -chitins. Signals labelled with asterisk are side bands from the rotor.

different hydrogen bonding network in the two polymorphs (Gardner & Blackwell, 1975).

The structure of  $\alpha$ -chitin, as determined by Minke & Blackwell, 1978, through X-ray analysis, involves a very specific set of hydrogen bonds. A statistical mixture of  $\text{CH}_2\text{OH}$  conformations was suggested (Mima *et al.*, 1982) with half of the  $\text{CH}_2\text{OH}$  groups, close to the *gt* conformation, forming intermolecular hydrogen bonds with OH-6 groups of the neighboring chain, and the other half, close to the *tg* conformation, forming intramolecular hydrogen bonds with the  $\text{C}=\text{O}$  groups of the next residue along the same chain. The two populations of  $\text{CH}_2\text{OH}$  groups originate in the IR spectrum of  $\alpha$ -chitin bands at  $3479$  and  $3444\text{ cm}^{-1}$ , respectively.  $\beta$ -chitin showed in this region a single broad band centered at  $3444\text{ cm}^{-1}$ ; its  $\text{CH}_2\text{OH}$  groups were suggested to be intra-sheets, linked to  $\text{C}=\text{O}$  groups (Gardner & Blackwell, 1975).

Deuteration of both  $\alpha$ - and  $\beta$ -chitins caused in a low-frequency shift ( $3430\text{ cm}^{-1}$ ) of the intermolecular OH stretching vibration mode.

To obtain more detailed information, FSD and FD techniques were applied for resolution enhancement of the OH and Amide I bands in the IR spectrum. These band-narrowing methods allow the resolution of the complex OH and amide bands into their components whose underlying areas, derived from curve fitting analysis, reflect relative populations of various conformational states assigned to individual bands (Byler & Susi, 1986; Mantsch *et al.*, 1986).

The deconvoluted spectra in the OH and NH stretching region confirm the complexity of the spectrum of  $\alpha$ -chitin (Fig. 2), where the band broadening may be caused by the existence of a number of energetically non-equivalent hydrogen bonds as well as of various interactions among conformationally nonuniform chains. Figure 2 also compares the

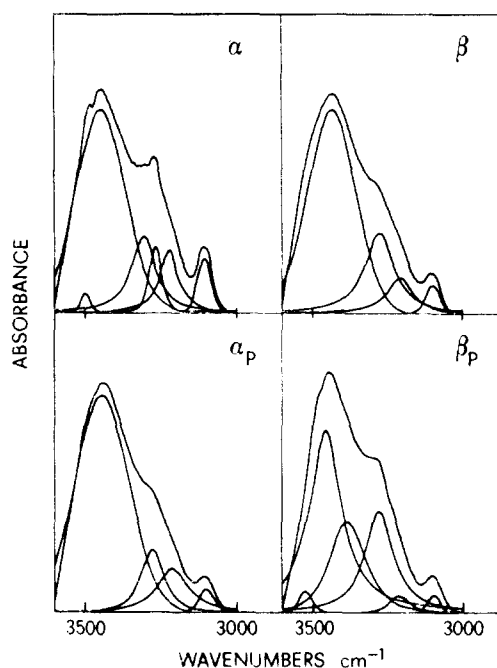


Fig. 2. Deconvoluted IR spectra ( $3600$ – $3000\text{ cm}^{-1}$ ) and curve fit of  $\alpha$ -,  $\beta$ -,  $\alpha_p$ - and  $\beta_p$ -chitins.

deconvoluted spectrum in the same region of  $\beta$ -chitin which displays less bands than  $\alpha$ -chitin. The frequency of each band depends on the nature of the hydrogen bonds; both in  $\alpha$ - and in  $\beta$ -chitin some overlapping bands, representing non-ordered and ordered structural features, are present with different intensities. However, in  $\beta$ -form the broader OH and NH bands are expected to represent a larger number of conformational states.

The Amide I band corresponds primarily to  $\text{C}=\text{O}$  stretching vibrations coupled to in-plane NH bending and CN stretching modes (Miyazawa *et al.*, 1956). The frequency of this vibration depends on the secondary

structure of the polymer, hence on the specific nature of the hydrogen bonding involving C=O and NH groups. In this work we consider only the Amide I vibration, which is more conformation-sensitive than Amide II or III vibration (Surewicz & Mantsh, 1987). As previously reported (Pearson *et al.*, 1960; Mima *et al.*, 1982),  $\alpha$ -chitin shows a splitting of the amide I vibration at 1660–1623  $\text{cm}^{-1}$ , the former component being assigned to the stretching of C=O groups hydrogen bonded to NH groups of the neighboring chain, and the second one to the stretching of the C=O groups hydrogen bonded both to the NH and to OH—6 groups of the same chain.

The occurrence of two non-equivalent populations of C=O groups in  $\alpha$ -chitin is clearly indicated also by the Raman spectrum (Fig. 3). In contrast, the IR and Raman bands associated with Amide I vibration of  $\beta$ -chitin consist only of a broad, complex band centered at higher frequency.

The deconvoluted IR spectrum and the corresponding band fitting procedure (Fig. 4) show that most typical feature of  $\alpha$ -chitin is the band at 1660  $\text{cm}^{-1}$  which disappears almost completely after deuteration and may thus be associated with conformational states of polymer involving intermolecular hydrogen bonding. The band at 1623  $\text{cm}^{-1}$ , resistant also to prolonged deuterium exchanges, is expected to be associated to an intramolecular hydrogen bond between C=O and NH groups. Besides the main component bands, two other components at 1674 and 1639  $\text{cm}^{-1}$  are present as shoulders. The latter are very likely due to some defects in the crystals of the small fibrils, as observed by X-ray analysis in most chitin specimens through the occurrence of a (001) reflection decreasing as the crystalline perfection increases (Minke & Blackwell, 1978). This is confirmed by the IR spectrum of an  $\alpha$ -chitin sample impregnated with a 5%  $\text{CH}_3\text{COOH}$  solution, successively flash treated. This treatment, which reduces the crystal perfection (Focher *et al.*, 1991), brings about a pronounced evidence of the aforementioned shoulders.

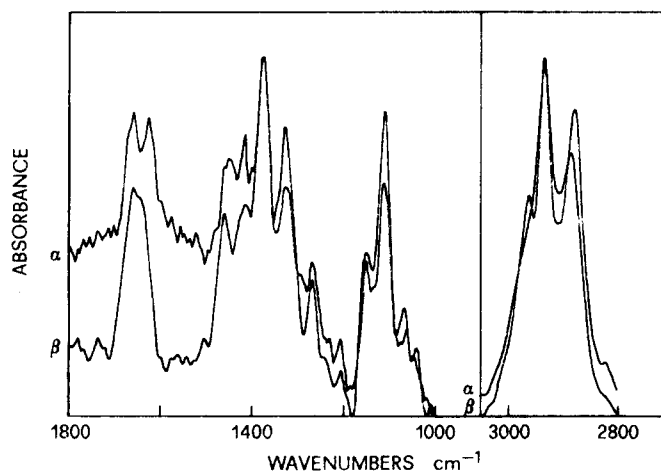


Fig. 3. FT-Raman spectra of  $\alpha$ - and  $\beta$ -chitins.

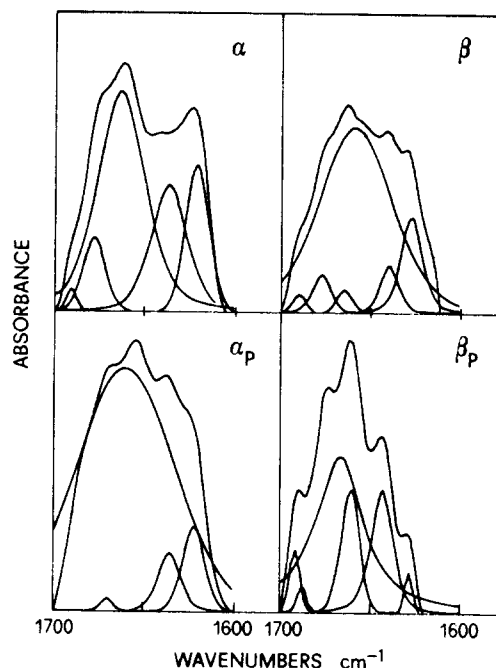


Fig. 4. Deconvoluted IR spectra (1700–1600  $\text{cm}^{-1}$ ) and curve fit of  $\alpha$ -,  $\beta$ -,  $\alpha_p$ - and  $\beta_p$ -chitins.

The fit of the Amide I band of  $\beta$ -chitin (Fig. 4) has some common features with that of  $\alpha$ -chitin. However, bands are centered at different wavenumbers and have different intensity ratios. These results are confirmed by the second derivative spectra.

The presence of different conformational states in the two polymorphs of chitin is also clearly indicated by CP-MAS spectra (Fig. 1). The C=O signal of  $\alpha$ -chitin at 175 ppm, exhibiting an asymmetric profile, proves the occurrence of two populations of acetamido groups. This is not observed for  $\beta$ -chitin, whose C=O signal was sharper and more symmetrical than that observed for the  $\alpha$ -form.

The involvement of the primary hydroxyl group in two kinds of hydrogen bonding network accounts for the IR and Raman vibration modes of  $\alpha$ - and  $\beta$ -polymorphs both in the CH stretching (3000–2600  $\text{cm}^{-1}$ ) and in the conformation sensitive region (1450–1420  $\text{cm}^{-1}$ ) (Cael *et al.*, 1974). The deconvoluted spectrum of  $\alpha$ -chitin (Fig. 5) shows five well resolved bands attributed to the asymmetric  $\text{CH}_3$  stretching (2963  $\text{cm}^{-1}$ ),  $\text{CH}_3$  symmetric and  $\text{CH}_2$  asymmetric stretching (2932  $\text{cm}^{-1}$ ), CH stretching (2908, 2874, 2891  $\text{cm}^{-1}$ ) and a shoulder at 2840  $\text{cm}^{-1}$  attributed to the  $\text{CH}_2$  symmetric stretching. The  $\beta$ -chitin spectrum in this region (Fig. 5) is less resolved, and the  $\text{CH}_3$  stretching band of amide groups appears as a shoulder. The same difference is observed also in the Raman spectrum (Fig. 3) suggesting, according to X-ray analysis, a distinct environment of the amide groups in the two polymorphs. On the other hand, the CP-MAS signal of  $\text{CH}_3$ , is, like the other signals of  $\beta$ -chitin, broader than the corresponding one of  $\alpha$ -chitin.

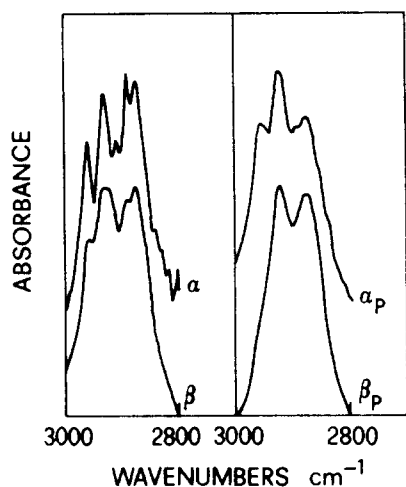


Fig. 5. Deconvoluted IR spectra (3000–2600  $\text{cm}^{-1}$ ) and curve fit of  $\alpha$ -,  $\beta$ -,  $\alpha_p$ - and  $\beta_p$ -chitins.

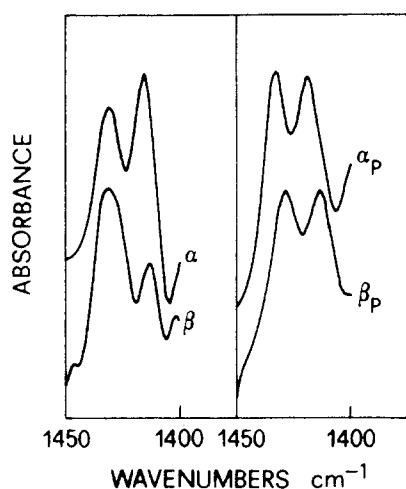


Fig. 6. Deconvoluted IR spectra (1450–1400  $\text{cm}^{-1}$ ) of  $\alpha$ -,  $\beta$ -,  $\alpha_p$ - and  $\beta_p$ -chitins.

In the  $\text{CH}_2$  bending region (1450–1420  $\text{cm}^{-1}$ ),  $\alpha$ -chitin shows (Fig. 6) a band at 1433  $\text{cm}^{-1}$ , weaker than for  $\beta$ -chitin, evidencing a different environment of the primary hydroxyl groups in the two cases. Similar differences were also observed for the band at 890  $\text{cm}^{-1}$ , due to vibrational modes involving the anomeric centers, and expected to be sensitive both to hydrogen bonding and to characteristics of the glycosidic bond.

A weaker band at 1416  $\text{cm}^{-1}$  in the spectrum of  $\beta$ -chitin (Fig. 6), assigned to  $\text{CH}_3$  deformation, is in line with the above observations concerning the  $\text{CH}_3$  group vibration. Since the intensity difference of the  $\text{CH}_2$  bending bands is shown also in the corresponding Raman spectra (Fig. 3), this band may be used to monitor conformational differences of the primary hydroxyl groups in the chitin polymorphs, hence distinct interchain interactions.

### Precipitated $\alpha$ - and $\beta$ -chitins

The X-ray diffraction patterns of the precipitated  $\alpha_p$ - and  $\beta_p$ -chitins (not shown) suggest that the precipitation treatment smoothes out the structural differences of the parent polymers. The CP-MAS  $^{13}\text{C}$ -NMR spectra (Fig. 1) show a general broadening of the signals in comparison with the spectra of the parent polymers, suggesting the occurrence of a less ordered packing of chains. However, in the case of  $\beta$ -chitin, the precipitation treatment induces a remarkable modification of the native structure, showing separate signals for carbons C—3 and C—5, as observed for native  $\alpha$ -chitin. Similar behavior is also observed in the deconvoluted IR spectra, mainly in the region of hydrogen-bonded OH and NH groups (Fig. 2), wherein precipitation  $\beta$ -chitin exhibits a profile apparently close to that of  $\alpha$ -chitin also for the NH vibration at 3269  $\text{cm}^{-1}$ . This feature is clearly shown in the CH stretching (Fig. 5) and in the Amide I (Fig. 6) regions. The rearrangement of the hydrogen bonding network, caused by the precipitation treatment, induces in the spectrum of  $\alpha$ -chitin the occurrence of a single, very broad band suggesting the presence of a composite of unresolved components in random conformations. The spectrum of regenerated  $\beta$ -chitin in the Amide I region (Fig. 6) shows a well-defined multicomponent feature constituted by a broad band representing domains of distinct conformations and indicating a deep modification of the metastable structure of the parent polymer. The new feature results in a different architecture with respect to that of  $\alpha$ -chitin.

### CONCLUSIONS

- Spectroscopic techniques are suitable for differentiating the structure of chitin polymorphs included the precipitates from solution. In particular, FDS and FD computational methods for the resolution-enhancement of broad infrared bands, provide the basis for an estimation of various conformational states of polysaccharide chains.
- Unlike the 'regeneration' of cellulose, which brings about a new polymorph, the chitin recovered from solutions has an essentially crystalline form as the chitin prior to solution. However, the precipitates from  $\alpha$ -chitin are somewhat more disordered than those from  $\beta$ -chitin, which are more ordered than the original metastable polysaccharide.

### ACKNOWLEDGEMENTS

The authors express their appreciation to Prof. B. Casu for helpful discussions. Thanks are due to M. T. Palma, C. Cosentino and M. Canetti for experimental work.

This work was supported by a grant from Italian

National Research Council (CNR), through the Finalized Project 'Chimica Fine II'.

## REFERENCES

- Abbott, T. P., Palmer, D. M., Gordon, S. H. & Bagby, M. O. (1988). *J. Wood Chem. Technol.*, **8**, 1-28.
- Abdul-Haleem, M. & Parker, K. D. (1976). *Z. Naturforsch.*, **31c**, 383-8.
- Blackwell, J. (1969). *Biopolymers*, **7**, 281-98.
- Byler, D. M. & Susi, H. (1986). *Biopolymers*, **25**, 469-87.
- Cael, J. J., Koenig, J. L. & Blackwell, J. (1974). *Carbohydr. Res.*, **32**, 72-91.
- Calstrom, D. (1957). *J. Biophys. Biochem. Cytol.*, **3**, 669-83.
- Darmon, S. E. & Rudall, K. M. (1950). *Discussion Faraday Soc.*, **9**, 251-60.
- Dweltz, N. E. (1960). *Biochim. Biophys. Acta*, **44**, 416-35.
- Focher, B., Naggi, A., Torri, G., Terbojevich, M. & Cosani, A. (1992). *Carbohydr. Polym.* (in press).
- Focher, B., Beltrame, P. L., Naggi, A. & Torri, G. (1990). *Carbohydr. Polymers*, **12**, 405-18.
- Gagnaire, D., Saint-Germain, J., Vincendon, M. (1982). *Makromol. Chemie*, **183**, 593-601.
- Gardner, K. H. & Blackwell, J. (1975). *Biopolymers*, **14**, 1581-95.
- Gow, N. A. R., Gooday, G. W., Russel, J. D. & Wilson, M. J. (1987). *Carbohydr. Res.*, **165**, 105-10.
- Griffiths, P. R. (1983). *Science*, **222**, 297-302.
- Kauppinen, J. K., Moffat, D. J., Mantsch, H. H. & Cameron, D. (1981). *Anal. Chem.*, **53**, 1454-7.
- Mantsch, H. H., Casal, H. L. & Jones, N. (1986). *Spectroscopy of Biological Systems*, ed. R. J. H. Clark & R. E. Hilster, J. Wiley & Sons, New York.
- Mima, S., Iwamoto, R. & Yoshikawa, S. (1982). *Proceedings of the Second International Conference of Chitin and Chitosan*, Sapporo, Japan, p. 21.
- Minke, R. & Blackwell, J. (1978). *J. Mol. Biol.*, **120**, 167-81.
- Miyazawa, T., Shimanouchi, T. & Mizushima, S. I. (1956). *J. Chem. Phys.*, **24**, 408-18.
- Muzzarelli, R. A. A. (1977). *Chitin*, Pergamon Press, Oxford.
- Muzzarelli, R. A. A., Jeuniaux, C. & Gooday, G. W. (1986). *Chitin in Nature and Technology*, Plenum Press, New York.
- Pearson, F. G., Marchessault, R. H. & Liang, C. Y. (1960). *J. Polym. Sci.*, **43**, 101-16.
- Ramakrishnam, C. & Prasad, N. (1972). *Biochim. Biophys. Acta*, **261**, 129-35.
- Rudall, K. M. (1963). *Adv. Insect. Physiol.*, **1**, 257-313.
- Saito, H., Tabeta, R. & Ogawa, K. (1987). *Macromolecules*, **20**, 2424-30.
- Savitzky, A. & Golay, M. J. E. (1964). *Anal. Chem.*, **36**, 1627-39.
- Surewicz, W. K. & Mantsch, H. H. (1987). *Biochem. Biophys. Acta*, **952**, 115-30.
- Susi, H. & Byler, D. M. (1983). *Biochem. Biophys. Res. Comm.*, **115**, 391-7.
- Terbojevich, M., Carraro, C., Cosani, A. & Marsano, E. (1988). *Carbohydr. Res.*, **180**, 73-86.
- Thomas, G. J. Jr. & Agard, D. A. (1984). *Biophys. J.*, **46**, 753-68.